

Using bedform migration and orientation to infer sediment transport pathways in a sandy braided river

C.A. Unsworth & A.P. Nicholas

Geography, College of Life and Environmental Sciences, University of Exeter, Exeter EX4 4RJ, UK

P.J. Ashworth & C.J. Simpson

Division of Geography and Geology, School of Environment and Technology, University of Brighton, Brighton, Sussex BN2 4GJ, UK

J.L. Best

Departments of Geology, Geography, Mechanical Science and Engineering and Ven Te Chow Hydrosystems Laboratory, University of Illinois at Urbana-Champaign, 1301 W. Green St., Urbana, IL 61801, USA

S.N. Lane

Institute of Earth Surface Dynamics, Faculté des Géosciences et de l'Environnement, Université de Lausanne, Bâtiment Géopolis, Lausanne, Switzerland.

D.R. Parsons

Department of Geography, Environment and Earth Sciences, Faculty of Science, University of Hull, Hull, HU6 7RX, UK

G.H. Sambrook Smith

School of Geography, Earth, Environmental Sciences, University of Birmingham, Edgbaston, Birmingham B15 2TT, UK

ABSTRACT:

The morphodynamics of sandy braided rivers are complicated by the presence of bedforms, which alter the spatial distribution of momentum, shear and sediment transport. These effects are not understood well and are typically simplified in morphodynamic models. This paper presents acoustic Doppler current profiler (aDcp) measurements of flow, and unmanned aerial vehicle (UAV) photogrammetric surveys of a 600 m reach of the sandy braided South Saskatchewan River, Canada. The response of alluvial bedforms to varying flow direction, bed-slope and sediment availability is examined, and the use of bedform crestline tracking to estimate sediment transport direction is discussed.

1 INTRODUCTION

Despite recent progress in modeling the morphology and dynamics of sand-bed rivers (e.g., Schuurman *et al.*, 2013), such models still contain significant uncertainties and limitations. In the case of 2D depth-averaged models that are suitable for simulating river evolution over timescales of decades to centuries, a key weakness is their neglect or simplification of processes associated with the ubiquitous presence of alluvial bedforms in sand-bed rivers.

Numerous studies have measured and modeled the effects of alluvial bedforms on flow and sediment transport in channels with simple morphological configurations (e.g., Naqshband *et al.*, 2015). However, current understanding of how such bedforms influence spatial patterns of flow and sediment transport in channels with more complex

morphology (e.g., channel-wide bars, converging or diverging flow and scour pools) remains limited. Attaining a more complete understanding of how bedform-scale and bar-scale topography interact to control the routing of water and sediment within natural channels is thus a pre-requisite for developing improved parameterizations of bedform effects within 2D morphodynamic models.

Of critical importance is the direction and magnitude of bedload sediment transport via bedform migration under the presence of lateral bed slopes and cross-channel flows. Bedform crest orientation and bedload transport direction are not consistent under lateral slopes due to gravitational deflection of sediment downslope (Hooke 1975; Dietrich *et al.*, 1979; Parker & Andrews 1985), leading to rotation of bedform crestlines (Talmon *et al.* 1995; Sieben & Talmon 2011).

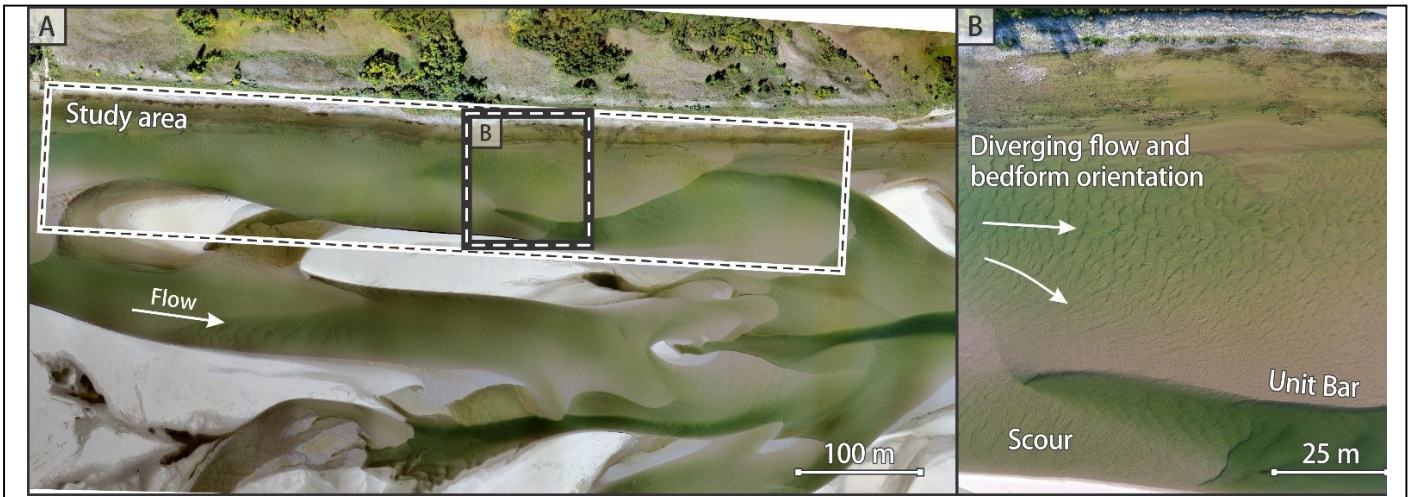


Figure 1a. Aerial photograph of the South Saskatchewan River from September, Canada 2015 at a discharge of $60 \text{ m}^3\text{s}^{-1}$. The near-zero suspended sediment and turbidity allows aerial photographs to reveal river bathymetry as well as emergent bar tops and banks. Flow depths reach 3 m in the scours; Figure 1b. Close up UAV image of bedform orientation change over a unit bar. Flow depths range from 1.2 m in the scour hole to 0.1 m on the unit bar top.

Bedform crest orientation is also spatially linked to the migration rate of nearby bedforms. Thus, a cross-channel gradient in crest migration rate can cause slower migrating crestlines to be stretched downstream (e.g., at bar fronts). In addition, rates of sediment transport and bedform migration are likely to be affected by spatial lag effects associated with supply limited transport. This may be important in braided rivers that are characterized by a mixture of sediment rich and starved areas, for example, due to deposition of sediment onto bar slip faces.

Herein, we present results from a study using a combination of high-resolution UAV and aDcp field data measurements of the South Saskatchewan River, Canada (*cf.* Parker *et al.*, 2013), that seeks to quantify and understand how topography and flow interact to control the routing of sediment within braided river channels.

2 FIELD DATA COLLECTION

Data quantifying channel morphology, flow and sediment transport were collected within a 600 m by 100 m reach of the river in 2015 (Figure 1a). The study reach is characterized by a range of bedform scales, with dunes up to 0.3 m high and 3 m in length, and unit bars up to 0.9 m high and > 50 m wide (Figure 1b). The study reach was bounded by an emergent bar on the true right and by vegetated floodplain on the true left. Mean 3D flow velocity data were acquired by repeated measurement at cross-sections 30 m apart to derive an average cross section flow structure using a SonTek M9 aDcp (Figure 2a).

The spatial distribution and orientation of bedforms was quantified with repeated UAV surveys, whereby images were rectified and merged using Structure from Motion photogrammetry using the software Pix4D (Figures 1-4). A low resolution ($1 \text{ m} \times 0.5 \text{ m}$) DEM was produced by interpolating the aDcp depth soundings and used to estimate the mean bed slope (Figure 3).

3 RESULTS

The depth-averaged velocity field within the study reach, monitored using the aDcp, is shown in Figure 2a. Key features of the flow include: (1) flow upstream of the bar converging into a depression; (2) expanding flow downstream of this scour; (3) the presence of a thalweg near the true left bank of the channel; and (4) topographic forcing of flow over the bar producing strong lateral flow toward the true right bank.

Bedform crests were identified on the aerial imagery and crest orientations were measured (arrows in Figure 2b are perpendicular to the bedform crests and directed downstream). At point 1 the bedform crest orientation appears strongly controlled by bed-slope of the scour (Figure 2b). In contrast, the thalweg on the true left side of the bar has no significant lateral slope, and bedform crests are aligned with the flow direction (point 3, Figure 2b). Between the thalweg at point 3 and the bar edge at point 4, crest orientation remains consistent despite greater lateral flow (Figures 2a & 2b). However, at point 2, crests are oriented at ~ 90 degrees to the crests in the thalweg.

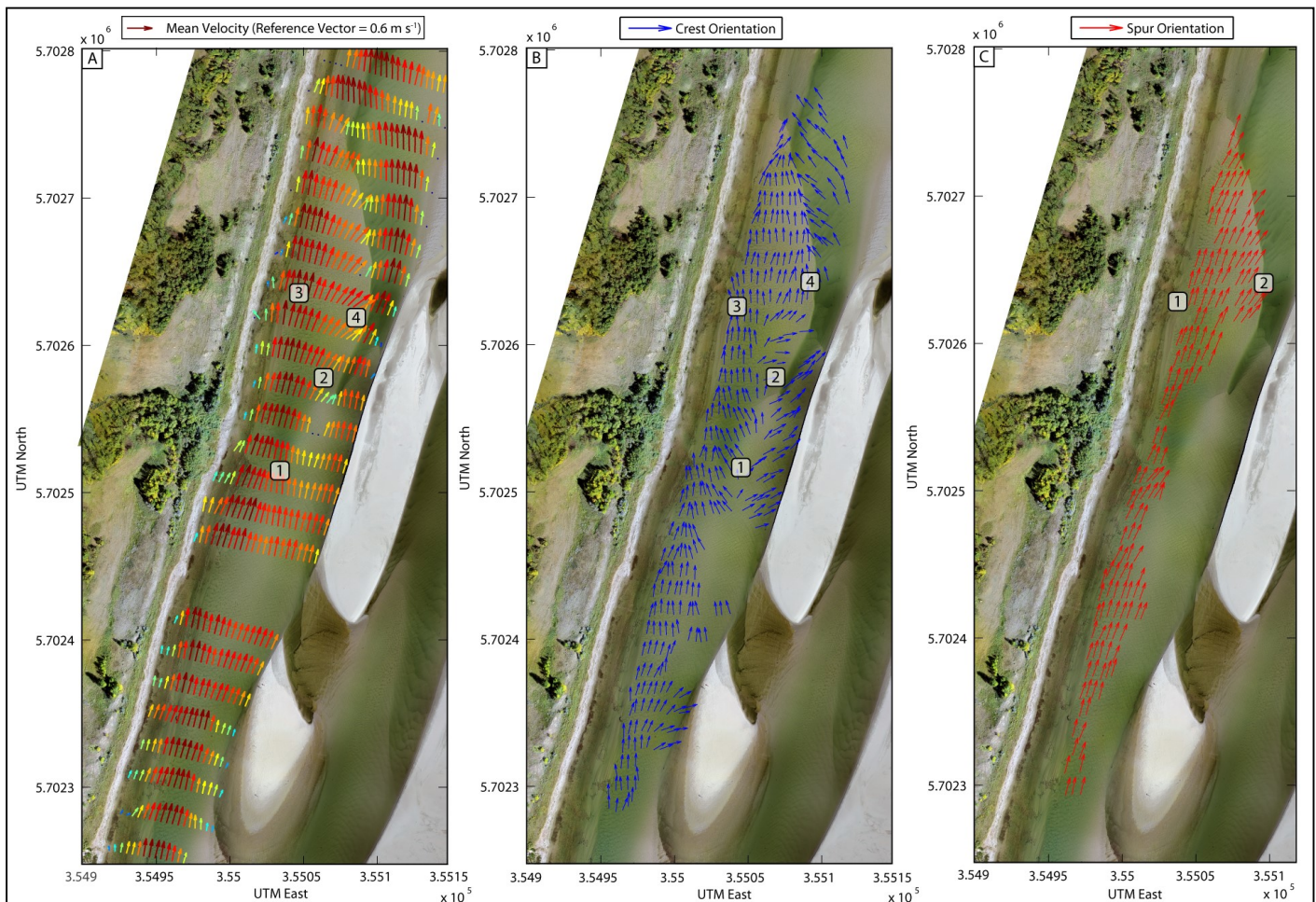


Figure 2a. aDcp mean flow vectors plotted on top of a geo-rectified mosaic of images taken from the UAV. Figure 2b. The dune crest orientation is displayed as arrows perpendicular to bedform crestlines. Figure 2c. The spur orientation is displayed across the UAV image. Gaps in 2b and 2c represent areas where no clear bedform crests or spurs could be identified.

Bedform spurs, which exist as a scour on dune stoss slopes, were mapped across the survey reach (Figure 2c). In contrast to the orientation of bedform crests (Figure 2b, points 3 to 4), the orientation of spurs is affected by the increasing lateral flow across the bar (Figure 2c, points 1 to 2).

The end of the bar is detailed in Figure 3a. There is a thalweg on the bar (point 1), where flow and bedform orientation is aligned closely. When the thalweg migrates toward the bar edge (at point 2) flow is deflected around gravel at the bank edge (point 3). Despite this deflection of the thalweg and some flow passing over the gravel, bedform and mean flow direction in the thalweg remain aligned.

As flow depth decreases across the bar from the thalweg toward the bar edge (points 1 to 4 in Figure 3a) a greater across stream (left to right) mean flow occurs. This is matched in the orientation of the bedform spurs, yet the bedform crests tend to be aligned towards the thalweg (in line with the bed slope). Figure 3b displays the start of the bar, associated scour pool and superimposed unit-bar (at point 4).

From point 1 to 2 in Figure 3b, bedform orientation changes from being closely in-line with the downstream flow (point 1) to orientated toward the bar edge and scour pool at near point 2. This is despite the flow depth decreasing from true left to right and in contrast to the minimal effect of bed-slope and flow on bedform orientation seen in Figure 3a. The orientation of bedforms at point 2 gradually changes downstream to become aligned at an angle that lines between the flow and bed slope directions at point 3 in Figure 3b.

Figure 4 displays the orientation of bedforms across two surveys separated by 5 hours on a patch of bed at the upstream end of the survey. The true left shows bedforms that have a mixture of 2D and 3D crestlines (Figure 4a). These crestlines do not migrate downstream uniformly, with bedform splitting, amalgamation and defect overpassing introducing variance in bedform crestlines, shape and orientation through time (Figure 4b). Bedform crestlines on the true right display highly 2D crestlines, rotated clockwise by ~30 degrees with respect to the flow direction and the bedforms on the true left. The bedforms on the true left migrated on average 1.5 m,

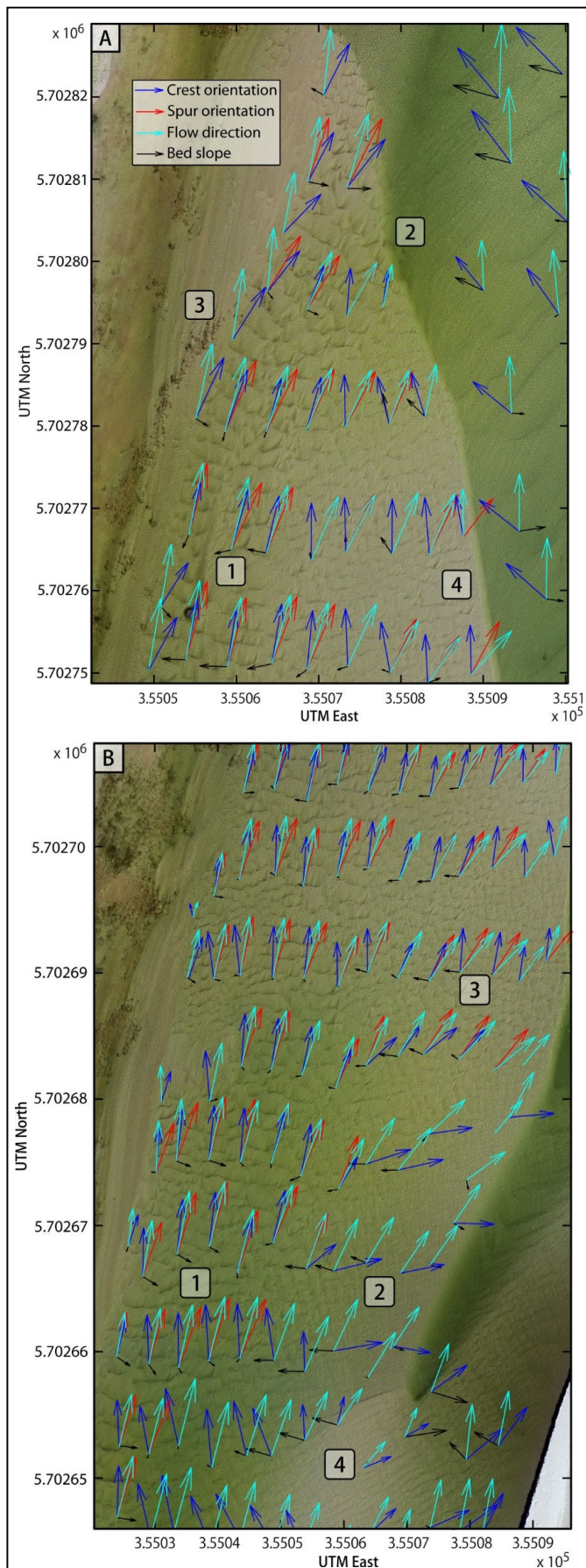


Figure 3. Close ups of the study reach with vectors showing the orientation of the mean flow (light blue), bedform crests (dark blue), spurs (red), and bed slope (black, with arrows pointing down-slope). Crest and spur vectors are scaled to the nearest mean velocity magnitude.

whilst bedform on the right migrated on average 1 m over 5 hours. Bedform crestlines and their orientations were mapped and averaged over a grid that had a minimum downstream spacing of 2 bedforms, so capturing the same bedforms through time (Figures 4c and 4d).

Due to the transience in bedform crestlines through time, estimating sediment transport direction via tracking bedform crestlines requires either spatial or temporal averaging to find the mean bedform orientations; thus removing any autogenic bedform features. High and low resolution spatial averaging was performed to illustrate this in Figures 4c & 4d, with spatial averaging of 5 x 3 m and 8 x 8 m, respectively. The greater spatial averaging in Figure 4d results in a closer match in bedform orientation between surveys. The bedforms crestlines on the true right display a consistent orientation through time, pointing toward the bank side. Yet the flow direction over these bedforms is downstream rather than in the direction perpendicular to the bedform crestlines (Figure 4b). As the bed slope decreases from the bottom to the top right of Figure 4d, bedform crest orientations both become oriented toward to the mean flow direction.

4 DISCUSSION

Effects of bed-slope and flow direction on bedform orientation.

It has been reported previously that bedforms reduce the effect of lateral flow on bedload transport direction in meander bends (Dietrich *et al.*, 1979), as bedform orientation is also affected by the overall bed slope because of gravitational deflection of sediment transport in the dune troughs (Sieben & Talmon, 2011). This effect is illustrated in Figure 3a, where bedform crestline orientations lie between that of the bed-slope and flow directions, indicating some sediment transport is down-slope. The spurs on the stoss slope of these bedforms are orientated to the flow direction, indicating a direct depth-average flow direction and sediment transport linkage on the dune stoss slope, constraining the possibility of downslope sediment transport direction to the bedform troughs. The result of these competing sediment transport directions is bedform crestlines that remain similarly orientated to dunes in the thalweg and lie between the bed-slope and flow directions. In bedload dominated conditions (as here) the sediment transport direction is a function of bed-slope, flow direction and dune

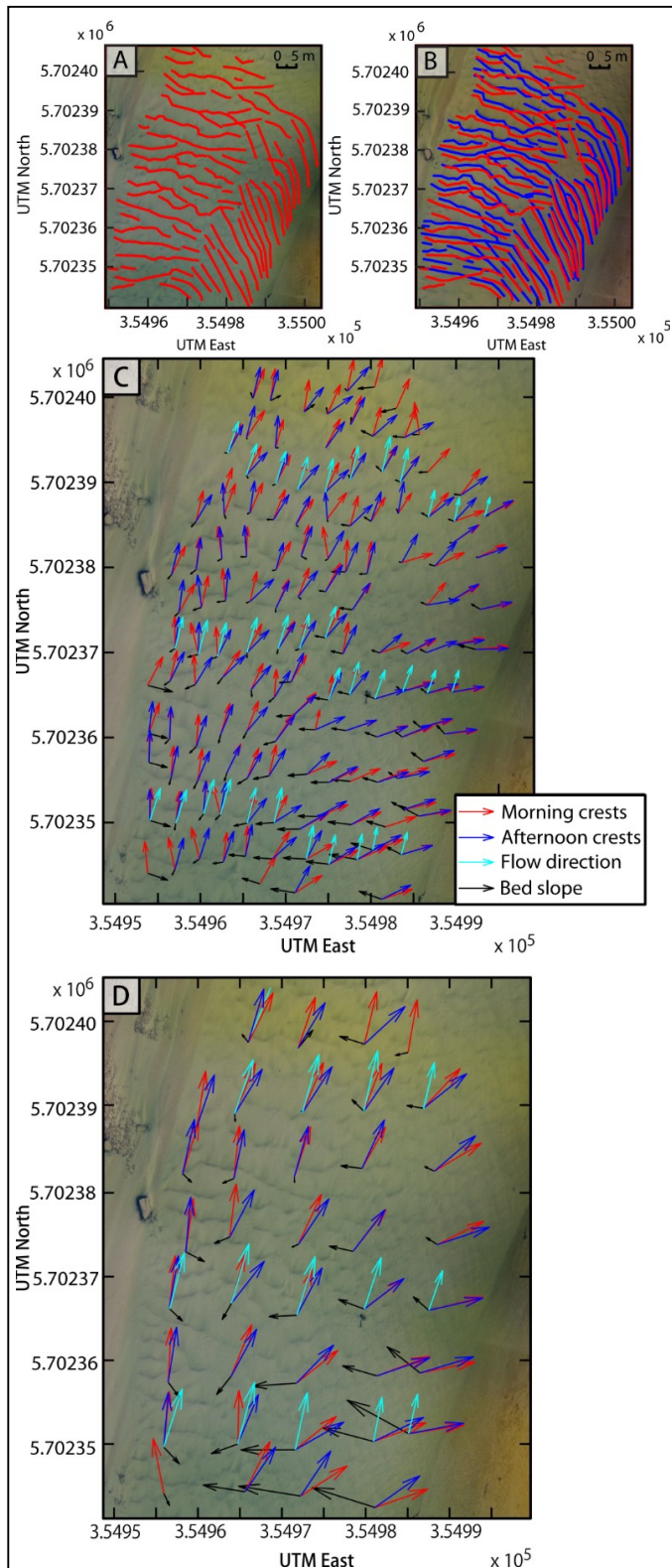


Figure 4. Bedform crestlines mapped for two UAV surveys red = morning survey, dark blue = afternoon survey. Panel b has both morning and afternoon crestlines to illustrate migration. Panels c and d display high and low (respectively) resolution spatial average of bedform orientation directions with flow and bed slope directions. Crest orientation arrows are scaled to the nearest mean velocity magnitude.

height. Consequently, it becomes feasible to estimate sediment transport direction using bedform crests.

Effect of sediment supply on bedform orientation.

Figure 3b displays a case where bedform crest lines are oriented so that lee slopes migrate up-slope toward the scour pool (point 2 in Figure 3b). It is interpreted that sediment travelling over the superimposed bar, upstream of point 2, will be deposited onto the superimposed bar lee face (near point 4), rather than continuously transported downstream; producing a shadowing effect around point 2. Because of this reduction in streamline sediment supply, the source of sediment around point 2 in Figure 3b is constrained to the thalweg. Consequently, bedforms migrate from the thalweg and spread into the shadowed region downstream of the superimposed unit bar, rather than following the flow direction or bed-slope. This indicates that bedform crestlines that do not lie between the bed-slope and flow directions (as outlined above) may still be indicative of sediment transport direction

Effects of bed-slope and flow direction on bedform migration

Figure 4 demonstrates that crestline three-dimensionality and autogenics impact on the temporal and spatial consistency of the bedform crests at the true left of the bar, producing crest orientation variability between surveys that is localized and not representative of the flow or mean bed-slope. This inherent transience requires averaging in order to estimate sediment transport direction. On the true right, the high bed-slope (absent on the true left) and lower migration rate appears to have reduced bedform transience leading to consistent bedform orientation between surveys at both resolutions tested (Figure 4c & 4d). The lateral difference in migration rate from true left to right has led to bedform crestlines becoming elongated downstream, suggesting sediment transport towards the bankside, under the assumption that transport is perpendicular to the crestlines. Yet these same bedform crestlines migrated downstream (Figure 4b) and not toward the emergent bank to the east (i.e. perpendicular to the bedform crestlines).

These results illustrate that when using bedform crestlines to measure sediment transport routing, factors such as bed slope, flow direction, depth and location of sediment supply need to be accounted for.

Because the orientation of bedform crestlines is not solely manifest from flow forced sediment transport along the dune stoss and gravitational deflection of sediment on the lee side slip-face. Bedform crestline orientation is also dependent upon spatially dependent factors such as a spatially variable sediment transport rate. This is illustrated in the warping of bedform crestlines from the thalweg to bar edges in Figures 3b and 4d, which give the impression that sediment transport is not in the same direction as mean flow or gravity.

5 CONCLUSIONS

A combined UAV and aDcp survey was undertaken on the South Saskatchewan River, Canada, revealing the detailed flow structure and morphology of the sandy braided river. It was shown that under full sediment availability and spatially uniform migration rates, bedform crestline orientation is affected by flow and bed-slope directions. Under supply limited conditions, such as downstream of a bar slip-face, bedform crestline orientation is dependent upon the location of sediment supply, rather than flow direction or bed-slope.

Small scale bedform autogenics and crestline three-dimensionality obscures the sediment transport direction. Therefore, spatial (or temporal) averaging is required to estimate the true sediment transport direction. Spatially disparate crestline migration rates produce bedform orientations that do not match their migration direction.

Further work is ongoing to measure the spatial distribution of sediment transport rate with respect to the behavior described above, and to quantify the effects of flow and bed-slope magnitude and direction on the spatial distribution of sediment transport under lateral slopes.

6 ACKNOWLEDGEMENTS

We thank Bill Varve for access to his land for the fieldwork and Dwight Thies for assistance with UAV flying. This research was supported by grants NE/L00738X/1 (A. P. Nicholas), NE/L005662/1 (P.J. Ashworth), NE/L00450X/1 (D.R. Parsons) and NE/L005441/1 (G. Sambrook Smith) from the UK Natural Environment Research Council (NERC). We thank Pix4D for the provision of an educational license for the Structure from Motion photogrammetry.

7 REFERENCES

- Dietrich, W.E., Smith, J.D. & Dunne, T. (1979). Flow and sediment transport in a sand bedded meander. *The Journal of Geology*, 87(3), pp.305–315.
- Hooke, R.L.B., 1975. Distribution of sediment transport and shear stress in a meander bend. *The Journal of Geology*, 83(5), pp.543–565.
- Naqshband, S., van Duin, O., Ribberink, J., and Hulscher, S. (2015) Modeling river dune development and dune transition to upper stage plane bed. *Earth Surface Processes and Landforms*, doi: 10.1002/esp.3789.
- Parker, G. & Andrews, E.D., 1985. Sorting of bed load sediment by flow in meander bends. *Water Resources Research*, 21(9), pp.1361–1373.
<http://doi.org/10.1029/WR021i009p01361>
- Parker, N.O., Sambrook Smith, G. H., Ashworth, P. J., Best, J. L., Lane, S N., Lunt, I.A., Simpson, C.J. Thomas, R.E. (2013). Quantification of the relationship between surface morphodynamics and subsurface sedimentological product in sandy braided rivers. *Sedimentology*, 60(3), pp.820–839. doi: 10.1111/j.1365-3091.2012.01364.x
- Schuurman, F., Marra, W. A. & Kleinhans, M.G., (2013). Physics-based modelling of large braided sand-bed rivers: Bar pattern formation, dynamics, and sensitivity. *Journal of Geophysical Research: Earth Surface*, 118(4), pp.2509–2527. doi: 10.1002/2013JF002896
- Sieben, J. & Talmon, A.M., 2011. Bed-load transport in obliquely dune-covered riverbeds. *Journal of Hydraulic Research*, 49(3), pp.317–324. doi 10.1080/00221686.2011.566252
- Talmon, A.M., Struiksma, N. & Mierlo, M.C.L.M. Van, 1995. Laboratory measurements of the direction of sediment transport on transverse alluvial-bed slopes. *Journal of Hydraulic Research*, 33(4), pp.495–517.
doi:10.1080/00221689509498657